Basic Cs-Pt/MCM-41 catalysts: Synthesis, characterization and activity in *n*-hexane conversion

J. Blanchard [a], K. Fajerwerg [a], M. Breysse [a], P. Beaunier [a], M.F. Ribeiro [b], J.M. Silva [c] and P. Massiani [a]*

[a] *Laboratoire de Réactivité de Surface, UMR 7609, CNRS, Université Pierre et Marie Curie, 4 place Jussieu, 75252 Paris cedex 05, France*
[b] *Departamento de Engenharia Química, Instituto Superior Técnico, Av. Rovisco Pais, 1049-001 Lisboa, Portugal*
[c] *Departamento de Engenharia Química, Instituto Superior de Engenharia de Lisboa, Av. Cons. Emídio Navarro, 1949-014 Lisboa, Portugal*

Received 2 May 2002; accepted 4 July 2002

Cs-Pt/MCM-41 catalysts with basic character have been prepared by selective adsorption of $Pt(NH_3)_4(OH)_2$ at pH = 8 on pure silica MCM-41 followed by incipient-wetness impregnation of $CsNO_3$, then oxidation and reduction. The influence of the amount of Cs (0, 2 and 4 wt%) on the size of the reduced Pt particles and on their catalytic behavior in the conversion of *n*-hexane has been investigated. Whatever the Pt content (0.7 or 2.0 wt% Pt), the addition of Cs results in a higher Pt dispersion, a higher initial activity and a higher selectivity for aromatization. On the more basic Pt-richest MCM-41 sample (4 wt% Cs, 2 wt% Pt) the selectivity to benzene reaches values close to those obtained on Cs-enriched Pt/Cs-BEA zeolite. However, the catalytic stability is lower. The catalytic trends are discussed in view of the physicochemical properties of the solids determined by chemical analysis, N_2 physisorption, XRD and TEM before and after catalytic test.

KEY WORDS: MCM-41; basicity; caesium; aromatization; nanoparticles; platinum.

1. Introduction

In recent years, a growing amount of attention has been paid to basic porous oxides due to their specific performances as new heterogeneous catalysts (fine chemistry) [1,2] or as new supports for active phases. One example is that of the industrial Pt/KL zeolite, which attracted strong interest in the 1980s owing to its high aromatization behavior in the conversion of *n*-paraffins [3]. The numerous research works conducted to explain the specific properties of Pt in basic KL have led to three main hypotheses that have been reviewed recently [4,5]. They are (i) a steric effect related to the channel geometry [6–8], (ii) an electronic enrichment of the metal particles by interaction with the basic KL support [9], and (iii) the very small size of the platinum clusters, which may change the electronic structure and thus the catalytic behavior of the Pt surface atoms [10]. The particle-size effect has been confirmed by showing that the Pt(111) terraces are the most active surfaces for both aromatization and terminal hydrogenolysis [11]. The influence of the basicity of the support on the catalytic activity of Pt in the conversion of *n*-paraffins has also been investigated using zeolitic supports other than KL [12], as well as non-zeolitic oxides such as SiO_2 [13] and Mg(Al)O [14]. Some authors [15] have reported that the presence of K^+ or Mg^+ additives in a neutral (non-acid) catalyst promotes aromatization of *n*-hexane.

* To whom correspondence should be addressed.
E-mail: massiani@ccr.jussieu.fr

Recently, we have compared the characteristics of Pt particles in Pt/alkali-BEA catalysts in which the basicity of the support was increased either by decreasing the electronegativity of the counter alkali cation [16,17] or by exchanging progressively the Na cations by Cs ones [18]. We have shown that an effect of basicity is to stabilize the metal species by generating stronger metal–support interactions [19], a consequence being a higher Pt dispersion after reduction [17,18]. We have also observed that the metal dispersion could be further raised by incorporating excess Cs in the Cs-exchanged BEA support [20]. The Pt nanoparticles with sizes $\leq$10 Å thus obtained showed properties close to those already reported for Pt/KL, and we proposed that this reaction can be taken as a test reaction to identify high metal dispersions in Pt-supported catalysts [20].

The addition of Cs in excess as compared to the cationic exchange capacity of a zeolite is known to generate strongly basic Cs_2O clusters dispersed in the microporosity [21,22]. Recently, the increase of the basicity by the addition of Cs has also been reported for non-zeolitic oxides such as MgO [23–24] and SiO_2 [25]. Furthermore, recent publications have reported on the introduction of caesium in the porosity of ordered mesoporous MCM-41. On the one hand, Perez *et al.* [26] have observed that the impregnation of MCM-41 supports with Cs acetate followed by calcination causes severe damage to the structure, especially in the case of Al-containing materials. On the other hand, Kloetstra and van Bekkum [27,28] have shown that Cs-exchanged, as well as Cs-impregnated MCM-41, are active basic catalysts for the Knoevenagel condensation.

1011-372X/02/1100-0221/0

One advantage of ordered mesoporous oxides as compared to disordered ones is their well-controlled porosity [29]. They also show high surface area, which allows one to achieve a high dispersion of the active phase. Moreover, their surface properties, as for instance the Cs/Si ratio, can be easily varied by post-synthesis treatment. Finally, their larger pore size [30] compared to zeolites could prevent pore blocking by bulky Cs cations.

The aforementioned advantages of mesoporous materials prompted us to extend our study of the behavior of Pt in Pt/Cs-BEA to the case of Pt/MCM-41 basified by the addition of Cs. This could help to identify further the roles of basicity and porosity in the formation of Pt nanoparticles and contribute to a better understanding of their reactivity in the conversion of *n*-hexane. To this purpose, we have prepared Cs-impregnated Pt/MCM-41 catalysts containing Cs (0, 2 and 4 wt%) and Pt (0.7 and 2.0 wt%), and have characterized them by N_2 physisorption, XRD and TEM. The physicochemical properties of the samples are discussed at each step of the preparation, and their catalytic behaviors in the conversion of *n*-hexane are compared to those of basic zeolitic Pt/Cs-BEA [31] taken as a reference.

2. Experimental

2.1. Materials

Synthesis of MCM-41. The parent silica molecular sieve with MCM-41 structure was synthesized according to the procedure described by Kim *et al.* [32]. This synthesis, which includes three pH adjustments and the addition of salt after a first heating period, improves greatly the stability of the MCM-41 material toward water. 58.6 g of colloidal silica (Ludox HS40 from Dupont, 40 wt% SiO_2) was added to 192 g of a 1 M NaOH solution under stirring at 75 °C and this mixture was left at the same temperature under stirring until a clear solution was obtained. This solution was cooled to room temperature and added dropwise to an aqueous solution of hexadecytrimethylammonium chloride (64 g of HTACl 25 wt% in water (Aldrich) mixed with 198 ml of water). The white mixture was transferred into a polypropylene bottle and kept in an oven at 95 °C for 24 h. After this first heating period, the mixture was cooled to room temperature, pH was adjusted to 10 with a 30% acetic acid-water solution and the mixture was heated again at 95 °C for 24 h. After this second heating period, 8.7 g of NaCl was added under stirring to the mixture. The pH adjustment procedure was repeated after a third heating period of 10 days and a fourth heating period of one day. After that, the precipitate was filtered and dried overnight in an oven at 90 °C. The surfactant was removed by a 2 h washing of the precipitate with a 0.1 M solution of NH_4Cl in ethanol at 78 °C (50 ml per g of precipitate), followed by a calcination under air flow (100 ml min^{-1} g^{-1}) at 550 °C (heating rate 1 °C min^{-1}) for 5 h.

Introduction of Pt. The driving force for the adsorption of Pt in solution is the electrostatic interaction of $[Pt(NH_3)_4]^{2+}$ with the silica surface. Thus, the choice of the pH is very significant since it should be high enough to favor the formation of $Si–O^-$ (ion-exchange sites) at the surface, but not too high to avoid a dissolution of the silica which would induce a collapse of the MCM-41 structure. pH = 8 seems to be a good compromise since at this pH the dissolution of silica is very slow but the surface charge is high enough to favor the interaction with cationic species [33]. Samples Pt_xMCM, where $x = 0.7$ (respectively 2) represents the wt% of Pt in the calcined solids, were prepared as follows: 70 μl (respectively 200 μl) of an aqueous tetraminoplatinum (II) hydroxide solution ($Pt(NH_3)_4(OH)_2$, 10 wt% Pt in water) were mixed with 100 ml of distilled water. 1 g of previously calcined MCM-41 was added and the pH was adjusted to 8 by adding NH_4OH upon stirring for approximately 10 min. The mixture was left under stirring for 3 h and the white precipitate was recovered by filtration, washed with water, rinsed with ethanol and dried overnight at 90 °C.

Addition of Cs. $CsNO_3$ was chosen as the Cs precursor in order to ensure the neutrality of the impregnation solution and the easy decomposition upon calcination in air. Increasing amounts of Cs (0, 2 or 4 wt%) were incorporated in the Pt/MCM-41 samples by incipient-wetness impregnation with appropriate amounts of an aqueous $CsNO_3$ solution ($CsNO_3$ 99% purchased from Fluka). The impregnated samples were dried at 90 °C overnight and finally calcined under O_2 flow (1 l min^{-1} g^{-1}) at 300 °C (heating rate of 1 °C min^{-1} until 200 °C and 0.25 °C min^{-1} until 300 °C) for 2 h before their characterization. They are henceforth referred to as samples Pt_xCs_yMCM, where x and y are the wt% of Pt and Cs in the calcined solids, respectively.

Reference samples. Sample $Pt_{0.7}$CsBEA (Si/Al = 15) containing 0.7 wt% of Pt was prepared as detailed elsewhere [31]. Its Cs content (atomic Cs/Al ratio of 1.2) is slightly higher than that required for charge equilibrium (Cs/Al = 1), indicating the presence of a small excess of Cs (≅3 wt% among the total 13 wt% of Cs) in the Cs-BEA zeolitic support. Sample $Pt_1Cs_4SiO_2$ (1 wt% Pt, 4 wt% Cs) was prepared as described for Pt_xCs_yMCM, but using Aerosil 380 (Degussa, 380 m^2/g, non-porous silica) as support.

2.2. Characterization

The contents (wt%) of Cs and Pt in the calcined samples were measured by atomic absorption (Central Analysis Service of the CNRS, France).

X-Ray diffractograms were collected on a Siemens D 500 X-ray diffractometer (Cu K_α, wavelength = 1.54 Å).

The scanning range was set from 1.7 to 8° (2θ) with a step size of 0.02 s.

N_2 adsorption-desorption isotherms were obtained at −196 °C on a Micromeritics ASAP 2010 instrument, after outgassing the samples at 150 °C under a pressure of 10^{-3} Torr for 5 h. The pore sizes were evaluated from the desorption branch of the isotherm using the BJH model.

Transmission electron microscopy (TEM) of the microtomed catalysts was used to determine the size and the location of the Pt particles in the samples previously reduced in flowing H_2 ($4\,l\,h^{-1}\,g^{-1}$) at 500 °C (5 °C/min) for 5 h. The micrographs were examined on a JEOL-JEM 100 CXII apparatus. Bulk mesoporous materials were embedded in a resin and cured at 70 °C for two days. Ultrathin sections (approximately 70 nm) were cut from the embedded sample using a diamond knife (Leica Ultra Cut UCT). They were laid on carbon-coated copper grids.

Thermogravimetric (TG) analysis of the catalysts after reaction was performed on a Setaram TG-DSC92 thermobalance. The coke formed during catalytic measurements was burnt under air flow ($50\,ml\,min^{-1}$) in the 25–800 °C temperature range ($2\,°C\,min^{-1}$).

2.3. Catalytic measurements

The *n*-hexane conversion reaction was performed in a semi-continuous flow reactor, at 450 °C under a total pressure of 1 bar. The calcined samples were reduced *in situ* in a flow of H_2 ($4\,l\,h^{-1}\,g^{-1}$) at 500 °C (5 °C/min) for 5 h. The reaction feed consisted of a mixture of hydrogen and *n*-hexane (molar ratio $H_2/n\text{-}C_6 = 6$), which was homogenized in a preheated (80 °C) vaporizer. H_2 was used as the carrier gas and the space velocity was kept constant (WHSV = $15\,h^{-1}$). The reaction products were separated and identified by an on-line Hewlett-Packard chromatograph, equipped with a 50 m plot capillary column (PONA) and a flame ionization detector (FID). The reproducibility of the tests was estimated at ±5.0%. The results are reported as conversions (percent of *n*-hexane reacted) and product selectivities (weight of product divided by weight of *n*-hexane reacted, in percent).

3. Results and discussion

The procedure for the preparation of the Pt_xCs_yMCM samples was chosen to provide a stable mesoporous MCM-41 structure, easily tune the amount of incorporated Pt and Cs, and achieve a high Pt dispersion. The platinum contents (table 1) indicate that all the Pt atoms of the $Pt(NH_3)_4(OH)_2$ solution have been adsorbed onto the MCM-41 support during preparation, thus confirming that the experimental conditions used (pH = 8) favored electrostatic interactions between the MCM-41 surface and the metal precursor cations.

3.1. Structure of the Pt_xCs_yMCM samples.

The XRD pattern (figure 1(a)) and N_2 physisorption isotherm (figure 2(a)) of the support after removal of the surfactant by washing in the NH_4Cl/ethanol solution and calcination are characteristic of hexagonal mesoporous MCM-41, with well-defined (100), (110), (200) and (210) diffraction peaks, and a high surface area ($990\,m^2/g$, table 1).

The fact that the MCM-41 structure has been preserved upon successive additions of Pt and Cs is shown by the XRD and N_2 physisorption data. A typical evolution of the XRD pattern along the preparation steps (figure 1) shows that the diffraction peaks of the MCM-41 structure are still well identified after the introduction of Pt, in spite of a small decrease of the peak intensities (figure 1(b)), and the decrease is more pronounced for the Cs-impregnated sample for which the (210) diffraction is no more visible (figure 1(c)). This reveals a progressive distortion of the long-range ordering of the hexagonal structure. The latter is associated with a progressive decrease of both the total surface area and pore diameters, as shown by

Table 1
Physico-chemical properties of the samples.

Samples	Chemical analysis		N_2 physisorption before and *(after)* catalytic test			TEM average particle size (Å)
	Pt (wt%)	Cs (wt%)	Surface area (m^2/g)	Pore volume (cm^3/g)	Ø pores (Å)	
MCM-41	–	–	990	0.9	29	–
$Pt_{0.7}$MCM	0.7	0	874	0.80	27	18
Pt_2MCM	2.0	0	923 *(896)*	0.83 *(0.80)*	28 *(25)*	23
Pt_2Cs_2MCM	2.0	2.0	696	0.56	25	n.d.
$Pt_{0.7}Cs_4$MCM	0.7	3.6	763 *(647)*	0.66 *(0.48)*	25 *(22)*	13
Pt_2Cs_4MCM	2.0	3.8	791	0.68	27	15
$Pt_1Cs_4SiO_2$	1.0	4.0	≅300	–	non-porous	n.d.
$Pt_{0.7}$CsBEA	0.7	13*	450	0.16	<7	11

* Cs in reference $Pt_{0.7}$CsBEA includes exchangeable Cs^+ cations (≅10 wt%) and excess Cs (≅3 wt%).
n.d. Non-determined.

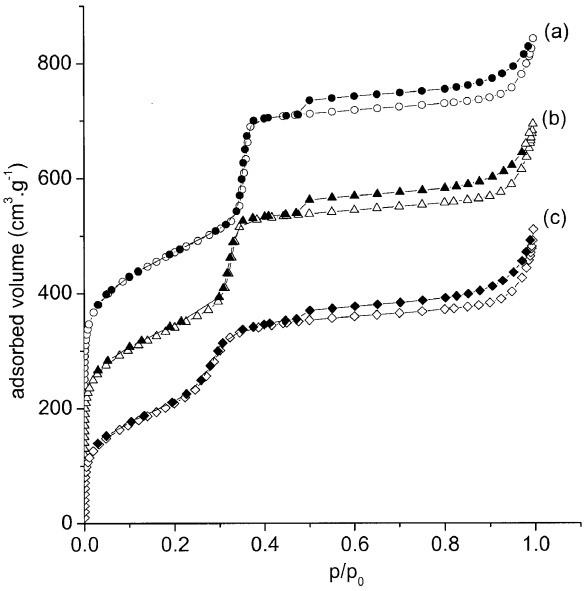

Figure 1. XRD patterns of (a) MCM-41, (b) $Pt_{0.7}$MCM and (c) $Pt_{0.7}Cs_4$MCM.

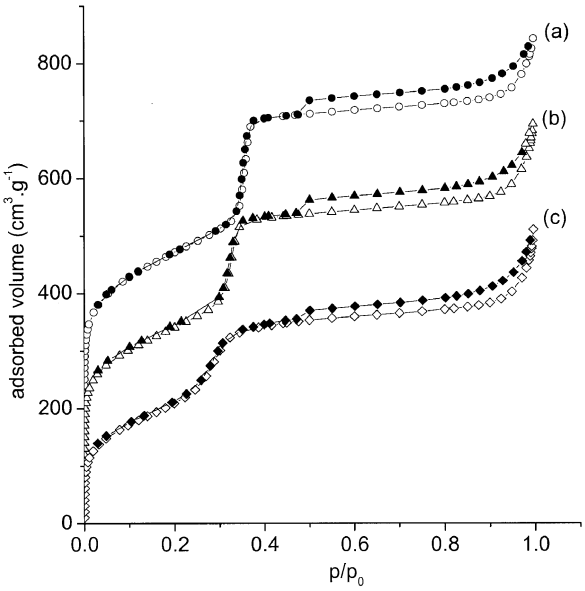

Figure 2. Nitrogen adsorption-desorption isotherm of (a) MCM-41, (b) $Pt_{0.7}$MCM and (c) $Pt_{0.7}Cs_4$MCM (open symbols denote adsorption, closed symbols desorption).

the N_2 physisorption data (figure 2 and table 1). The loss of order and porosity after impregnation with Cs could be due either to a pore blocking by Cs_2O clusters or to a partial collapse of the structure during this preparation step. In spite of these modifications, the surface area, pore volume and pore diameter remain important for all Pt_xCs_yMCM ($\geq 700\,m^2\,g^{-1}$, $\geq 0.55\,ml\,g^{-1}$ and ≥ 25 Å, respectively, table 1).

3.2. Platinum particle size

The Pt^0 particles after reduction have been characterized by TEM. A typical micrograph (reduced Pt_2Cs_4MCM, figure 3(A)) shows that the Pt particles are well dispersed inside the mesoporous channels. The distributions of the Pt particle sizes in the MCM-41-based and reference $Pt_{0.7}$CsBEA samples have been determined by measuring the diameters of about 200 particles (figure 4). The average sizes evaluated from these profiles are reported in table 1.

For most samples, the sizes of the metal particles detected by TEM are in the range 5–30 Å. A few larger particles (30–40 Å) are present in Cs-free Pt-rich Pt_2MCM (figure 4(b)), in which the average size (23 Å, table 1) is slightly higher than in Pt-poorer $Pt_{0.7}$MCM (18 Å). By contrast, the metal particles detected by TEM are significantly smaller in all Cs-containing Pt_xCs_yMCM (figure 4, table 1) and their sizes, in the range 5–15 Å, are close to those in reference $Pt_{0.7}$CsBEA containing excess Cs (figure 4(a)). Thus, Cs-impregnation results in an increase of the Pt dispersion which could be due, as already proposed for Pd/FAU [34] and Pt/Cs-BEA [17,18], to an interaction between the metal species and the basic Cs-enriched MCM-41 support along the successive preparation steps, leading to a stabilization of dispersed Pt. In the case of Pt/KL [35–37] and Pt/Cs-BEA [17], chemisorption and/or EXAFS have shown that additional Pt nanoparticles with sizes below the limit of detection of TEM could

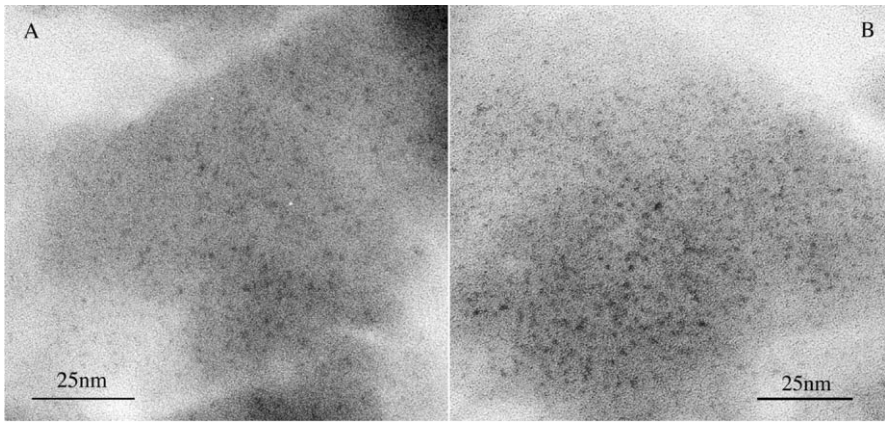

Figure 3. Transmission electron micrographs of reduced Pt_2Cs_4MCM. (A) Before and (B) after catalytic measurement.

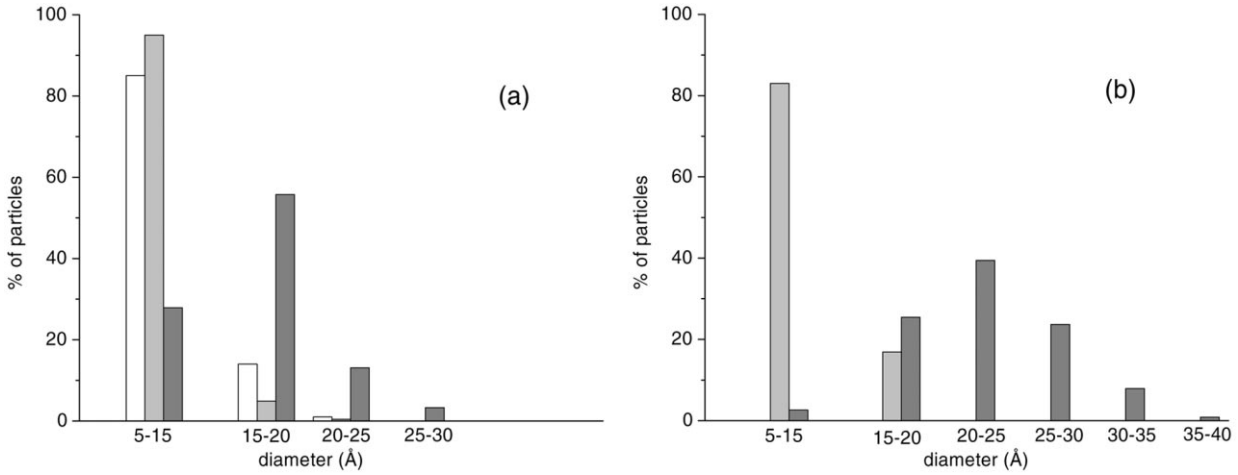

Figure 4. Particle-size distribution of (a) ■, $Pt_{0.7}$MCM; ■, $Pt_{0.7}Cs_4$MCM; □, $Pt_{0.7}$CsBEA and (b) ■, Pt_2MCM; ■, Pt_2Cs_4MCM.

also be present. Probably, this also takes place in the Pt_xCs_yMCM catalysts, as supported by preliminary EDS analyses, which suggest the presence of Pt in zones of the mesoporous support where particles are hardly identified by TEM. Additional experiments are being performed in order to clarify this point.

3.3. Catalytic results

The catalytic performances of the reduced Pt_xMCM and Pt_xCs_yMCM samples have been studied in the conversion of *n*-hexane, compared to those of the reference zeolitic ($Pt_{0.7}$CsBEA) and silica ($Pt_1Cs_4SiO_2$) catalysts. A blank test performed on a Pt-free MCM-41 containing 4 wt% of Cs showed no conversion, confirming the absence of active sites on the mesoporous support itself, on which no acidic sites are indeed expected (silica-based materials). In agreement, the main products of reaction formed during transformation of *n*-hexane on the Pt-containing MCM-41 catalysts corresponded to a conventional monofunctional reaction network occurring on metallic sites. They are C_1–C_5 hydrocarbons (hydrogenolysis products), 2- and 3-methylpentanes (skeletal isomers), methylcyclopentane (MCP, originating from hydrocyclization), benzene (main aromatization product) and other C_6 hydrocarbons containing olefins (present mainly on the deactivated catalysts). Table 2 details the conversions of *n*-hexane and selectivities to

Table 2
Conversion, selectivity to the main products, yields to aromatics, deactivation coefficients and terminal cracking index during transformation of *n*-hexane on the Pt-supported catalysts; coke content after catalytic experiment.

Catalysts	Conversion [a] (%)	Selectivity[a] (wt%)					Aromatic yields	$D_{conv.}$ [b] (%)	TGA weight loss (%) [c]	TCI [d]
		C_1–C_5	2MP + 3MP	MCP	C6 = +others	Aromatics				
$Pt_{0.7}$MCM	19 *(4)*	15 *(11)*	18 *(9)*	28 *(20)*	17 *(56)*	22 *(4)*	4.2 *(0.2)*	79	0.6	0.8
Pt_2MCM	25 *(9)*	20 *(18)*	18 *(10)*	21 *(17)*	16 *(41)*	25 *(14)*	6.3 *(1.3)*	64	–	1.1
Pt_2Cs_2MCM	28 –	8 –	24 –	12 –	21 –	35 –	9.8 --	–	2.1	2.9
$Pt_{0.7}Cs_4$MCM	25 *(4)*	7 *(4)*	30 *(8)*	14 *(16)*	20 *(69)*	29 *(3)*	7.3 *(0.1)*	84	2.2	1.8
Pt_2Cs_4MCM	34 *(7)*	9 *(11)*	23 *(12)*	18 *(19)*	8 *(39)*	35 *(19)*	11.9 *(1.3)*	79	–	2.2
$Pt_1Cs_4SiO_2$	23 *(3)*	9 *(8)*	31 *(11)*	12 *(8)*	22 *(66)*	26 *(7)*	6.0 *(0.2)*	87	0.2	2.1
$Pt_{0.7}$CsBEA	23 *(3)*	13 *(11)*	15 *(10)*	14 *(15)*	15 *(34)*	43 *(32)*	10.3 *(5.1)*	33	2.8	

[a] After 7 min and *(120 min)* time on stream.
[b] Deactivation coefficients $D_{conv.}(\%) = [(X_7 - X_{120})/X_7] \times 100$, where X_7 and X_{120} are the conversions of *n*-hexane at 7 and 120 min time on stream, respectively.
[c] TGA weight loss in the 150–350 °C temperature range.
[d] TCI (terminal cracking index) (*n*-C_5/*n*-C_4) determined at isoconversion (20%).

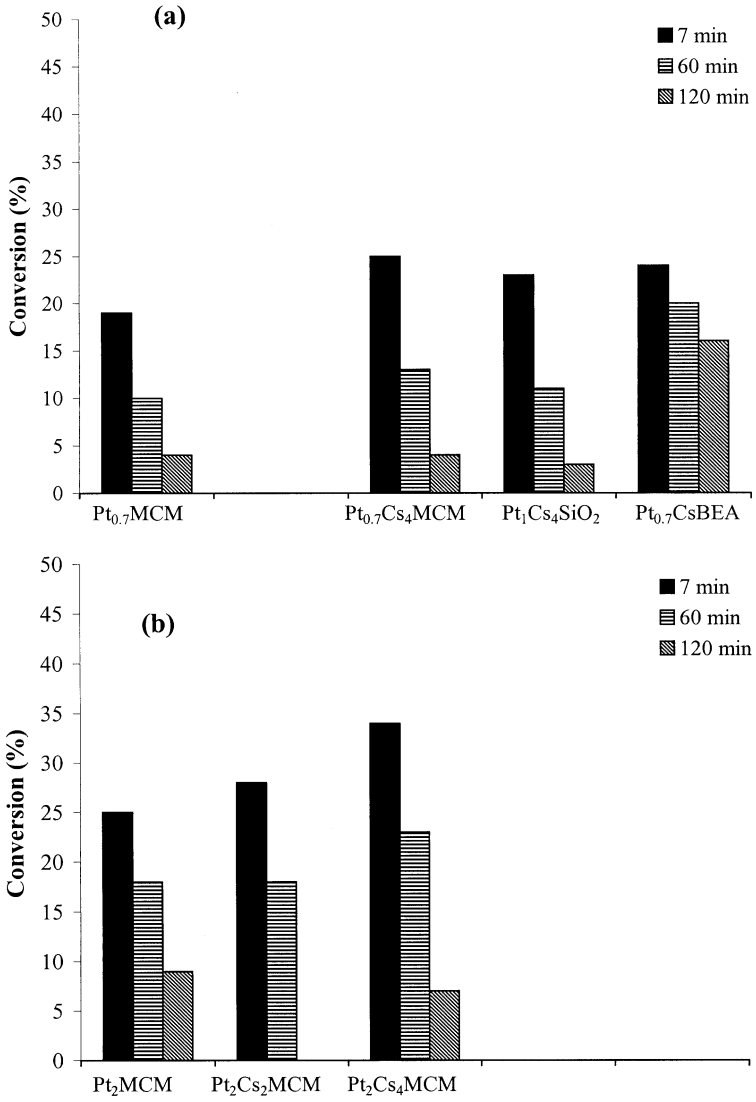

Figure 5. Conversions of *n*-hexane on the catalysts containing (a) 0.7 wt% Pt and (b) 2.0 wt% Pt.

the above products after 7 and 120 min time on stream for the various catalysts. It also reports the yields of aromatics and the coefficients of deactivation calculated as the ratios $D_{\text{conv.}} = [(X_7 - X_{120})/X_7] \times 100$, where X_7 and X_{120} are the conversions of *n*-hexane after 7 and 120 min time on stream, respectively. The conversions after 7, 60 and 120 min time on stream are also compared in figure 5.

3.3.1. Catalytic activity and stability

The comparison of the conversions after 7 min time on stream for the samples with low Pt loading (figure 5(a)) reveals that close conversions are obtained on all the Cs-enriched samples (*ca* 25% conversion on $Pt_{0.7}Cs_4$MCM, $Pt_{0.7}$CsBEA and $Pt_1Cs_4SiO_2$), whereas a lower conversion is reached on Cs-free $Pt_{0.7}$MCM (figure 5(a), table 2). Similarly, the addition of Cs in the 2 wt% Pt-containing MCM-41 catalyst induces an increase of the conversion at 7 min on stream, the latter being about one-third higher on Pt_2Cs_4MCM than on Pt_2MCM (figure 5(b), table 2). Such increases could be related to the higher Pt dispersions obtained in the Cs-impregnated samples.

The activity also increases with an increase of the Pt content in both the Pt_xMCM and Pt_xCs_yMCM series (compare data in figure 5(a) (0.7 wt% Pt) and figure 5(b) (2 wt% Pt)). Since the dispersion of Pt as evaluated by TEM is about the same for the two Pt contents, we could expect, for this monofunctional reaction, an increase in activity proportional to the platinum loading. However, as for Pt/Cs-BEA [20], no proportionality is observed for the mesoporous materials, as shown for instance by the X_7 value that is only one-third higher for Pt_2Cs_4MCM than for $Pt_{0.7}Cs_4$MCM (34% and 25%, respectively, table 2). The possibility that very small particles (<1 nm) not detected by TEM could be present in different amounts in the two samples, leading to different Pt dispersions, cannot be completely dispelled. However, the absence of correlation most

probably reflects the fact that a large part of the activity has already been lost during the first minutes of the run and that deactivation can vary from one sample to another, especially for catalysts containing different amounts of metal active phase.

The fact that deactivation took place during the catalytic runs is confirmed by the progressive decrease of the conversions on all the catalysts (figure 5). However, the activity loss is much more important on all the mesoporous (MCM-41-based) and non-porous (silica) catalysts than on the $Pt_{0.7}$CsBEA zeolite. Thus, all the Pt_xMCM and Pt_xCs_yMCM catalysts, and the $Pt_1Cs_4SiO_2$ reference, show a progressive and strong deactivation ($D_{conv.}$ around 80–85%) leading to a very low activity after 120 min time on stream, whereas the deactivation coefficient is two to three times lower for $Pt_{0.7}$CsBEA (table 2). This higher stability of the zeolitic catalyst agrees with the proposal made for Pt/KL that microporosity plays a role in the stability of the metallic sites during transformation of *n*-paraffins [13,38,39]. Furthermore, the low stability of $Pt_1Cs_4SiO_2$ is in line with the usual observation made on Pt/SiO_2 [15,40].

The important deactivation levels observed on the MCM-41-based catalysts can suggest (i) a sintering of the metallic particles, (ii) a pore blocking due to coke formation or to a collapse of the MCM-41 structure and/or (iii) a poisoning of the catalytic site through coke deposit. In order to discriminate between these hypotheses, representative samples have been characterized after catalytic run. Firstly, the comparison of the micrographs of Pt_2Cs_4MCM before and after test (figure 3) shows that the sizes of the Pt particles are comparable, indicating that no sintering visible by TEM occurred during reaction. If present, a particle-size effect would therefore require that very small Pt particles invisible by TEM be involved. Secondly, the N_2 physisorption data recorded after catalytic measurement for both $Pt_{0.7}Cs_4$MCM and Pt_2MCM (table 1) indicate that the surface area, pore size and pore volume are slightly lower after catalysis. However, the decrease seems too small (5–15%) to explain the high level of deactivation on the basis of a pore blocking solely. Another argument against this hypothesis is that pore blocking could not justify the low catalytic stability of non-porous Pt/silica. Therefore, it is probable that deactivation mainly takes place through inhibition of the metal active sites by coke deposit.

The amount of coke present in the solids after the catalytic runs has been characterized by TGA (weight loss during combustion of coke). Unexpectedly, the data (table 2) reveal that the coke amount is the highest in used $Pt_{0.7}$CsBEA, although this catalyst shows the lowest deactivation level (lowest $D_{conv.}$ value). Furthermore, we have observed, for both the mesoporous and the non-porous silica-based catalysts, the formation of yellow-brown liquid polyaromatics deposits in small amounts (not measured) at the exit of the reactor. These compounds, which are formed by cyclization/dehydrogenation reactions on these supports with low steric hindrance, lead to a progressive poisoning of the active metal sites by competitive adsorption/transformation/desorption between the polyaromatic precursor species and the *n*-hexane reactant. The formation of such bulky species is inhibited in the restricted BEA microporosity, which protects better the dispersed Pt active sites from deactivation. It has already been proposed that the Pt/zeolites with the lowest Pt dispersions and containing some Pt particles at the external surface of the zeolite crystallites undergo the greatest deactivation rates during *n*-heptane transformation, and that catalytic stability is related to the dispersion of very small Pt particles inside the zeolite channels [16,20]. Therefore, although the mesoporous structures make it possible to obtain catalysts with high Pt dispersions, their pore systems do not protect the active Pt particles as in zeolites, making them more sensitive to deactivation.

3.4. Aromatization properties

On most samples, the main products obtained after 7 min time on stream are aromatics, and the selectivity to these products decreases upon deactivation, the reaction then leading mostly to C_6 olefins produced by isomerization/dehydrogenation (table 2). The selectivities to aromatics are plotted in figure 6 as a function of the conversion. The latter was changed through deactivation occurring with time on stream. We have checked in a previous work [18], by changing the operating conditions, that the deactivation process does not modify the intrinsic selectivity behaviors with conversion. Table 2 details the selectivities to aromatics on all fresh and used catalysts.

As in the case of Pt/CsBEA [20], the impregnation of the Pt_xMCM catalysts with Cs induces a significant increase of the selectivity to aromatization. Thus, at isoconversion (20%), the selectivity to aromatics is about 1.4 times higher on Cs-enriched $Pt_{0.7}Cs_4$MCM than on Cs-free $Pt_{0.7}$MCM with same Pt loading, and it approaches that on $Pt_{0.7}$CsBEA (figure 6(a)). As for Pt/BEA [17,18], this increase seems to follow the progressive decrease of the average particle sizes from 18 Å ($Pt_{0.7}$MCM) to 13 Å ($Pt_{0.7}Cs_4$MCM), then 11 Å ($Pt_{0.7}$CsBEA). Similarly, for the samples of the MCM-41 series with 2 wt% Pt, the selectivity to aromatics increases with the addition of Cs (figure 6(b), table 2) and this increase is associated again with the decrease of the particle size, the effect being slightly more pronounced than above however. This is in line with the higher difference in particle size between Pt_2MCM and Pt_2Cs_4MCM (23 and 15 Å, respectively) than between $Pt_{0.7}$MCM and $Pt_{0.7}Cs_4$MCM (18 and 13 Å, respectively). Also, the increase of the selectivity to aromatics is progressive with Cs content, as illustrated for the Pt_2Cs_yMCM series (compare selectivities at isoconversion, figure 6(b)).

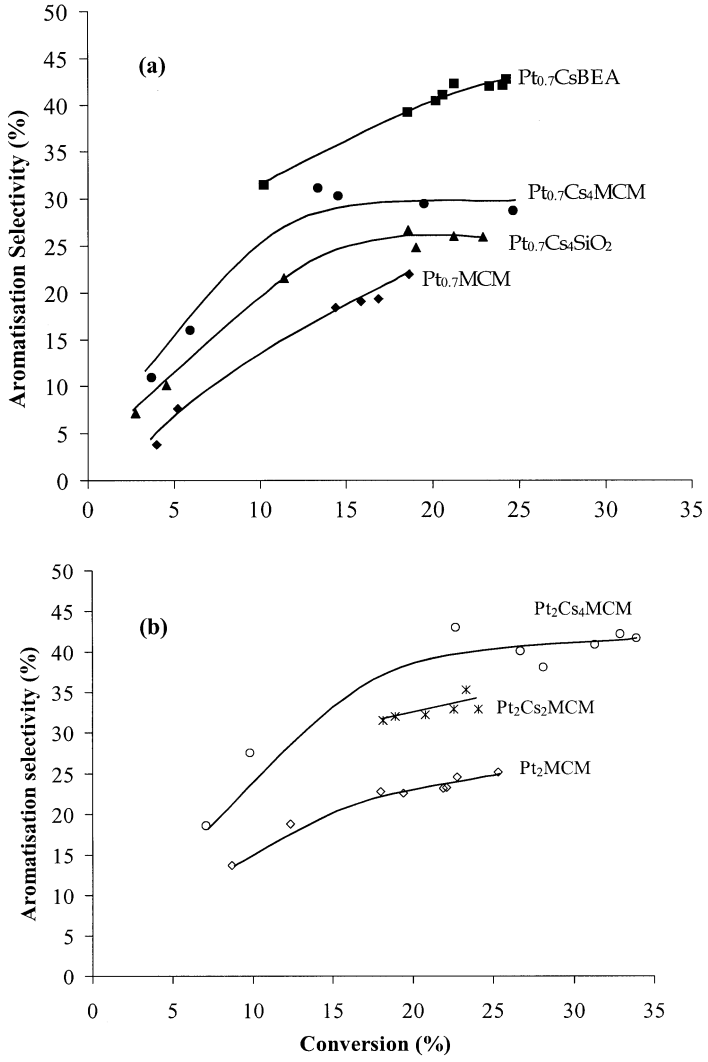

Figure 6. Selectivities to aromatics as a function of *n*-hexane conversion on the catalysts containing (a) 0.7 wt% Pt and (b) 2.0 wt% Pt.

In 1990, Tauster and Steger defined a terminal cracking index (TCI) as the molar ratio of the *n*-pentane to *n*-butane (C_5/C_4) formed during conversion of *n*-hexane [6]. Initially, these authors explained the high values observed on Pt/KL in terms of a molecular die effect involving the porous characteristics of the support. More recently, it has been proposed that this ratio is rather determined by the morphology of the Pt particle: the greater the particle size, the lower the TCI and the selectivity to aromatization [17,41]. In order to check if these trends also take place on the Pt-supported MCM-41 catalysts, we report the TCI values obtained at isoconversion (20%) for all samples (table 2). As expected, TCI is the lowest for the Cs-free catalysts ($\leq$1.1) with largest particles and lowest selectivities to aromatics. On the contrary, TCI is close to or higher than two for all Cs-containing samples, such high TCI values being in accordance with those reported for Pt-supported catalysts with high aromatization behavior [7,10].

4. Conclusions

MCM-41 samples containing increasing amounts of Pt and Cs have been prepared. XRD and/or N_2 physisorption data indicate that the mesoporous structure is well preserved after the introduction of Pt and Cs in the support, as well as after catalytic tests. The most interesting feature is that the impregnation of Cs on the Pt-containing samples prior to calcination results in a drastic decrease of the size of the metal particles after reduction, whatever the Pt content. The Pt nanoparticles detected by TEM in the reduced Cs-enriched Pt/MCM-41 catalysts thus have sizes in the range 5–15 Å, and they are as small as those identified in a Pt/Cs-BEA catalyst taken as a reference. Furthermore, the decrease in the size of the Pt particles upon addition of Cs in the MCM-41-based catalysts induces, as in the case of the zeolitic supports, an increase of the selectivity to aromatization. This indicates again that highly dispersed Pt plays a major role for product selectivities in this

reaction. Moreover, the porous system has a strong influence on catalytic stability and on the characteristics of deactivation in this reaction. Thus, the importance of the confined microporous channels for protecting the active metal sites during conversion of *n*-hexane is confirmed. However, such a requirement could be secondary for other catalytic reactions with different deactivation mechanisms for which Cs-enriched MCM-41 could represent a promising ordered support, with basic properties allowing the preparation of new catalysts for applications in which bulky reactants are involved.

Acknowledgments

Financial support from CNRS and ICCTI through international cooperation is gratefully acknowledged. The authors thank M.-D. Appay for the image treatment of the micrographs.

References

[1] H. Hattori, Appl. Catal. A: General 222 (2001) 247.
[2] J. Weitkamp, M. Hunger and U. Rymsa, Microp. and Mesop. Mater. 48 (2001) 255.
[3] J.R. Bernard, Proc. 5th Int. Zeol. Conf., ed. L.V.C. Rees (Heyden, London, 1980) p. 686.
[4] R.J. Davis, Heterogeneous Chemistry Reviews 1 (1994) 41.
[5] P. Meriaudeau and C. Naccache, Catal. Rev.-Sci. Eng. 39(1&2) (1997) 5.
[6] S.J. Tauster and J.J. Steger, J. Catal. 125 (1990) 387.
[7] G.S. Lane, F.S. Modica and J.T. Miller, J. Catal. 129 (1991) 145.
[8] E.G. Derouane and D.J. Vanderveken, Appl. Catal. 45 (1988) L15.
[9] C. Besoukhanova, J. Guidot, D. Barthomeuf, M. Breysse and J.R. Bernard, J. Chem. Soc., Farad. Trans. I 77 (1981) 1595.
[10] E. Mielczarski, S.B. Hong, R.J. Davis and M.E. Davis, J. Catal. 134 (1992) 359.
[11] M.S. Davis, F. Zaera and G.A. Somorjai, J. Catal. 85 (1984) 206.
[12] Z. Zhan, I. Manninger, Z. Paal and D. Barthomeuf, J. Catal. 147 (1994) 333.
[13] E. Iglesia and J.E. Baumgartner, Stud. Surf. Sci. Catal. 75 (1993) 993.
[14] R.J. Davis and E.G. Derouane, J. Catal. 132 (1991) 269.
[15] T. Fukunaga and V. Ponec, Appl. Catal. A 154 (1997) 207.
[16] F.J. Maldonado-Hodar, M.F. Ribeiro, J.M. Silva, A.P. Antunes and F.R. Ribeiro, J. Catal. 178 (1998) 1.
[17] F.J. Maldonado, T. Becue, J.M. Silva, M.F. Ribeiro, P. Massiani and M. Kermarec, J. Catal. 195 (2000) 342.
[18] T. Becue, F.J. Maldonado-Hodar, A.P. Antunes, J.M. Silva, M.F. Ribeiro, P. Massiani and M. Kermarec, J. Catal. 181 (1999) 244.
[19] A. Sauvage, M. Oberson de Souza, M.J. Peltre, P. Massiani and D. Barthomeuf, J. Chem. Soc., Chem. Com. 11 (1996) 1325.
[20] M. Taibi, A. Culic, P. Massiani, M. Lavergne, F. Villain, M.F. Ribeiro, C. Jia, J. Rigoreau and J.M. Silva, to be published.
[21] P.E. Hathaway and M.E. Davis, J. Catal. 116 (1989) 279.
[22] M. Lasperas, H. Cambon, D. Brunel, I. Rodriguez and P. Geneste, Microp. Mater. 1 (1993) 343.
[23] P. Thomasson, O.S. Tyagi, H. Knözinger, Appl. Catal. A: General 181 (1999) 181.
[24] R. Bal, B.B. Tope, S. Sivasanker, J. Mol. Catal. 1: Chemical 181 (2002) 161.
[25] E. Ruckenstein, A.Z. Khan, J. Catal. 141 (1993) 628.
[26] C.N. Perez, E. Moreno, C.A. Henriques, S. Valange, Z. Gabelica and J.L.F. Monteiro, Microp. Mesop. Mater. 41 (2000) 137.
[27] K.R. Kloetstra and H. van Bekkum, J. Chem. Soc., Chem. Commun. (1995) 1005.
[28] K.R. Kloetstra and H. van Bekkum, Stud. Surf. Sci. Catal. 105 (1997) 431.
[29] G. Oye, J. Sjoblom and M. Stocker, Advances in Colloid and Interface Science 89 Special Iss. SI (2001) 439.
[30] C.T. Kresge, M.E. Leonowicz, W.J. Roth, J.C. Vartul and J.S. Beck, Nature 359 (1992) 710.
[31] C. Jia, A.P. Antunes, J.M. Silva, M.F. Ribeiro, M. Lavergne, M. Kermarec and P. Massiani, Stud. Surf. Sci. Catal. 130C (2000) 2993.
[32] J.M. Kim, S. Jun and R. Ryoo, J. Phys. Chem. B 103 (1999) 6200.
[33] R.K. Iler, *The Chemistry of Silica* (Wiley-Interscience, New York, 1979).
[34] A. Sauvage, M. Oberson de Souza, M.J. Peltre, P. Massiani, D. Barthomeuf, J. Chem. Soc., Chem. Commun. (1996) 1325.
[35] M. Vaarkamp, J.T. Miller, F.S. Modica, G.S. Lane and D.C. Koningsberger, J. Catal. 138 (1992) 675.
[36] C. Dossi, R. Psaro, A. Bartsch, A. Fusi, L. Sordelli, R. Ugo, M. Bellatreccia, R. Zanoni and G. Vlaic, J. Catal. 145 (1994) 377.
[37] G. Jacobs, Firoz Ghadiali, Adriana Pisanu, Armando Borgna, W.E. Alvarez and D.E. Resasco, Applied Catalysis A: General 188(1–2) (1999) 79.
[38] S.B. Sharma, P. Ouraipryvan, H.A. Nair, P. Balaram, T.W. Root and J.A. Dumesic, J. Catal. 150 (1994) 234.
[39] G. Larsen and G.L. Haller, Catal. Lett. 17 (1993) 127.
[40] G. Jacobs, C.L. Padro and D.E. Resasco, J. Catal. 179 (1998) 43.
[41] P.V. Menacherry and G.L. Haller, J. Catal. 177 (1998) 175.